Diagn Interv Radiol 2012; 18:435–440

CHEST IMAGING

ORIGINAL ARTICLE

Contrast enhanced CT versus integrated PET-CT in pre-operative nodal staging of non-small cell lung cancer

Naim Ceylan, Sözen Doğan, Kenan Kocaçelebi, Recep Savaş, Alpaslan Çakan, Ufuk Çağrıcı

PURPOSE
The purpose of this study was to retrospectively evaluate the effectiveness of integrated positron emission tomography-computed tomography (PET-CT) in comparison with contrast enhanced CT (CE-CT) in pre-operative staging of non-small cell lung cancer (NSCLC) by using surgical and pathological findings as the reference standard.

MATERIALS AND METHODS
From August 2008 to August 2009, 57 consecutive patients (50 males and 7 females; mean age, 59 years; range, 38–79 years) with NSCLC underwent conventional pre-operative lung cancer staging using clinical data and CE-CT of the chest, and integrated whole-body fluorine-18 fluorodeoxyglucose PET-CT studies. Histopathological results served as the reference standard.

RESULTS
Forty-eight of the 57 patients (84%) had no lymph node involvement (N0), five (9%) were found to have N1 disease, and four (7%) had N2 disease. There was a significant difference between CE-CT and PET-CT for nodal staging of N0 disease ($P < 0.05$). Sensitivity, specificity, positive predictive value, negative predictive value, and accuracy of hilar and mediastinal lymph node staging were 56%, 73%, 28%, 90%, and 70%, with CE-CT, respectively; and 78%, 92%, 64%, 96%, and 89% with PET-CT, respectively.

CONCLUSION
Integrated PET-CT is more accurate than CE-CT for lymph node staging in NSCLC.

Key words: • positron emission tomography and computed tomography • lung cancer • lymph node

From the Departments of Radiology (N.C. ✉ *ceylannaim@gmail.com*, S.D., R.S.) and Thoracic Surgery (A.Ç., U.Ç.), Ege University School of Medicine, İzmir, Turkey; the Clinic of Nuclear Medicine (K.K.), Ege Sağlık Hospital, İzmir, Turkey.

Received 11 September 2011; revision requested 2 November 2011; revision received 1 January 2012; accepted 2 January 2012.

Published online 29 February 2012
DOI 10.4261/1305-3825.DIR.5100-11.2

Non-small cell lung cancer (NSCLC) accounts for approximately 75% to 85% of all newly diagnosed lung cancers (1). The optimal treatment of NSCLC relies on accurate disease staging, which is based on tumor size, regional nodal involvement, and the presence of metastasis. Correct evaluation of the presence or absence of metastases in mediastinal and hilar lymph nodes is a critical factor that may determine operability and long-term survival in patients with NSCLC. Surgical treatment can be expected in 70% of patients with N0 stage and up to 24% of patients with N2 stage; however, surgery is generally not indicated in patients with N3 stage cancer (2).

Although computed tomography (CT) is the most commonly used non-invasive imaging modality for the pre-operative evaluation of tumor size and the extent of invasion into adjacent structures, a number of reviews and meta-analyses have shown the limited reliability of CT in lymph node staging (3). The CT criteria for lymph node tumor involvement rely on the size or shape of the lymph nodes. Usually, 1 cm is used as the size criterion predicting tumor involvement in lymph nodes. However, normal sized lymph nodes may show metastases upon histological examination, and nodal enlargement may be due to reactive hyperplasia or other benign conditions (2). Rapid advances in multi-detector CT scanners allow a more detailed analysis of the lung parenchyma and mediastinal structures. As a consequence, nodal staging may be enhanced with CT.

Positron emission tomography (PET) with fluorine-18 fluorodeoxyglucose (FDG) has been reported to improve identification of nodal metastasis. FDG PET images may be more sensitive than CT because alterations in tissue metabolism generally precede anatomical changes (4). Integrated PET-CT provides information about anatomy and metabolism by combining morphological CT data and functional PET data (5). However, false-positive PET-CT results in nodal staging have been shown in patients with co-existing inflammatory or infectious diseases, and PET-CT scanning may be unable to identify metastatic deposits in normal-sized lymph nodes because of its suboptimal spatial resolution (6, 7).

Several retrospective and prospective studies have investigated the effectiveness of CT and PET-CT in pre-operative nodal staging of NSCLC (8–13). However, conflicting conclusions have been reported in these studies. Thus, the aim of our study was to retrospectively evaluate the effectiveness of integrated PET-CT in pre-operative staging of NSCLC in comparison with contrast enhanced CT (CE-CT) by using surgical and pathological findings as the reference standard.

Materials and methods

Patient population

From August 2008 to August 2009, 57 consecutive patients (50 males and 7 females; mean age, 59 years) underwent surgery for pathologically

proven localized, clinically resectable NSCLC. All patients underwent conventional pre-operative lung cancer staging based on clinical data and CE-CT of the chest, and integrated whole-body FDG PET-CT studies. None of the patients had received radiation or chemotherapy prior to surgery. CE-CT was always carried out prior to the PET-CT. The mean time interval between the CE-CT and PET-CT was one week. PET-CT was performed within one week of surgery. Histopathological results served as the reference standard. Our Institutional Review Board does not require approval or informed consent from patients for retrospective studies such as ours.

Contrast-enhanced CT acquisition and scan analysis

Axial CT was performed using a 16-section multi-detector CT scanner (Aquilion TSX-101A, Toshiba Medical Systems Corporation, Tokyo, Japan) with the following scanning parameters: 250 mAs, 120 kV, pitch 1, 16×1 mm collimation, 1 mm reconstruction interval, and 1 mm reconstruction section thickness. Scans were obtained from the supraclavicular region to the middle of the kidneys during deep inspiration and a single breath-hold. Using an automatic injector (Ulrich Medizintechnik, Ulm, Germany), a 120 mL bolus of iodinated contrast material was injected through a catheter in the antecubital vein at a rate of 3 mL/s.

The thin-section CT image data were directly interfaced with our picture archiving and communication system (Syngo version V35, Siemens Healthcare, Erlangen, Germany), which displayed all image data on monitors. Bone, mediastinal, and lung window images were viewed on these monitors. CT scans were evaluated by two radiologists (S.D, N.C.) with five and 14 years of CT experience, who had to reach a consensus. The radiologists were blinded to the integrated PET-CT, surgical, and pathological findings. Tumor staging with CE-CT and PET-CT was based on the newly revised American Joint Committee on Cancer TNM system for the classification of lung cancer (14). Tumor staging was performed by considering the lesion size, involvement of the surrounding organs or chest wall, and distance of the primary tumor from the carina. Nodal stations were evaluated and allocated to 10 groups, according to the lymph node map definition for lung cancer staging proposed by Mountain and Dresler (15). Nodes with a short-axis diameter greater than 10 mm were defined as pathological. The presence of necrosis within a lymph node was considered a sign of malignancy, regardless of node size. If mediastinal or hilar nodes contained nodular or laminated calcifications, they were regarded as benign, irrespective of their size.

Integrated FDG PET-CT acquisition and scan analysis

All patients fasted for at least six hours before undergoing FDG PET-CT. After confirmation of a normal blood glucose level (less than 150 mg/dL) using a peripheral blood sample, patients received an intravenous injection of 370 MBq (10 mCi) of FDG and then rested for approximately 45 min prior to the scan. Integrated PET-CT was performed on a Philips Gemini System consisting of a PET scanner and a 16-slice CT scanner (Philips, Eindhoven, Netherlands). CT was performed from the head to the upper thigh using a standardized protocol involving 120 kV, 220 mAs, and a section thickness of 3.0 mm (which matched the PET image section thickness). Patients were allowed normal shallow respiration during the acquisition of CT and PET scans. To enhance the acquisition of diagnostic CT data, intravenous contrast agents were administered in all patient examinations. Immediately after CT, PET was performed in the identical axial field of view. The acquisition time for PET was 3 min per table position. CT data were resized from a 512×512 matrix to a 128×128 matrix to match the PET data and to enable image fusion and generation of CT transmission maps. PET image data sets were reconstructed iteratively using the ordered-subsets expectation-maximization algorithm and through segmented attenuation correction using the CT data. CT and PET data sets were displayed on a post-processing workstation in axial, coronal, and sagittal orientations and were fused with color-coded superimposition of the PET images on the CT images (Syngo version V35, Siemens Healthcare).

PET-CT images were evaluated by a chest radiologist with 20 years of experience in CT interpretation and six years of experience in PET-CT interpretation, and a nuclear medicine physician with five years of experience in PET-CT interpretation (R.S., K.K.). Both physicians were blinded to all findings on the CE-CT, which had been performed prior to PET-CT, as well as prior to obtaining all clinical and pathological results. Decisions about the findings were reached by consensus. The PET-CT images were evaluated qualitatively for regions of focally increased glucose metabolism, and quantitatively by determining standardized uptake values (SUV). The maximum standardized uptake value (SUV_{max}) of the primary tumor and lymph node were measured with a region-of-interest technique and calculated by the software according to standard formula. An increase in glucose uptake to a level greater than that in the surrounding tissue during qualitative analysis and an SUV of more than 2.5 were considered to be indicative of malignancy. Nodal stations were evaluated with the same lymph node map definition as the one used for CT scan interpretation. Hilar or mediastinal nodes with increased glucose uptake and with a distinct margin were considered to be positive for malignancy.

Surgical and histopathological analysis

Surgical staging included mediastinoscopic nodal sampling in two patients, video-assisted thoracoscopic surgery in two patients, and thoracotomy and lymph node dissection in all patients. Lung resection, including lobectomy and pneumonectomy with mediastinal lymph node dissection, were performed by two thoracic surgeons (A.C., U.C.) with 12 and 14 years of experience. The surgeons sampled all visible and palpable lymph nodes that were accessible in the hilum and mediastinum. All encountered lymph nodes were removed from American Thoracic Society lymph node map areas of 10R, 9, 8, 7, 4R, 3, and 2R in tumors of the right lung and from areas 10L, 9, 8, 7, 6, 5, and 4L of the left lung. A lung pathologist with 12 years of experience described the tumors and evaluated the nodes as numbered in the surgical field. A pathological stage was recorded for each patient, and a total of 470 lymph nodes were dissected in the 57 patients.

Statistical analysis

Statistical analyses were performed using a commercially available software (Statistical Package for Social Sciences version 16.0, SPSS Inc., Chicago, Illinois, USA). CE-CT and PET-CT findings were correlated with histopathological results. The sensitivity, specificity, positive predictive value, negative predictive value, and accuracy for evaluating hilar and mediastinal metastases were calculated for both CE-CT and PET-CT scans. Correlations between the SUV_{max} of lung cancer, tumor size and frequencies of lymph node metastasis were determined using the Pearson coefficient (r). Differences in imaging methods were evaluated with the Fisher exact test and the Mann-Whitney U test. A *P* value of less than 0.05 was considered to indicate a statistically significant difference.

Table 1. Patient and tumor characteristics (n=57)

Age (years)	
Mean±SD	59±15
Range	38–79
Gender, n (%)	
Male	50 (88)
Female	7 (12)
Site, n (%)	
Right upper lobe	28 (49)
Left upper lobe	11 (19)
Other	18 (31)
Tumor diameter (cm)	
Mean±SD	3.3±1.5
Range	0.6–11.5
Histology, n (%)	
Adenocarcinoma	27 (47)
Squamous cell	17 (30)
Other	13 (23)
Tumor SUV_{max}	
Mean±SD	7.2±4.5
Range	1–23
Pathological stage, n (%)	
IA	27 (47)
IB	16 (28)
IIA	1 (2)
IIB	10 (18)
IIIA	2 (4)
IIIB	1 (2)

SUV_{max}, maximum standardized uptake value; SD, standard deviation.

Results

Results of imaging studies and pathology

Table 1 summarizes clinical and pathological variables of the study group. A total of 57 patients (50 males and 7 females; mean age, 59±15 years; range, 38–79 years) were included in the study. Histological analysis demonstrated adenocarcinoma in 27 patients, squamous cell carcinoma in 17, large cell carcinoma in three, atypical carcinoid in three, pleomorphic carcinoma in two, adenosquamous cell carcinoma in one, mucoepidermoid carcinoma in one, adenoid cystic carcinoma in one, mucinous cystic tumor in one, and sarcomatoid carcinoma in one.

The tumor size was measured during pathological examination. The diameters of the primary lung tumors ranged from 0.6 to 11.5 cm with a mean value of 3.3±1.5 cm.

The distribution of overall staging (tumor and nodes) in the 57 patients, which was determined during pathological examination, included stage IA in 27 patients, stage IB in 16 patients, stage IIA in one patient, stage IIB in 10 patients, stage IIIA in two patients, and stage IIIB in one patient.

The SUV_{max} of the primary lung tumors ranged from 1 to 23 with a mean value of 7.2±4.5. FDG uptake in primary tumors was sufficient in 48 patients and lacking in nine. There was no significant difference in SUV_{max} between adenocarcinoma and squamous cell carcinoma ($P > 0.05$). The Pearson correlation coefficient was significant between the SUV_{max} of lung cancer and tumor size ($P < 0.05$, r=0.429).

Efficacy of multidetector CT and integrated PET-CT in diagnosing nodal metastasis

At pathological staging, 48 of the 57 patients (84%) did not have lymph node involvement (N0), five patients (9%) were found to have N1 disease, and four (7%) had N2 disease. A total of 470 lymph nodes were sampled. There were five highest mediastinal (nodal station 1), 25 upper paratracheal (station 2), 30 prevascular and retrotracheal (station 3), 119 lower paratracheal (station 4), 21 subaortic and aortopulmonary (station 5), 12 paraaortic (station 6), 108 subcarinal (station 7), eight paraesophageal (station 8), 11 pulmonary ligament (station 9), and 131 hilar (station 10) nodes, according to pathological examinations. Of these, 24 lymph nodes (5%) in nine patients proved to be positive for malignancy. Among the positive nodes, there were 15 hilar, one upper paratracheal, three lower paratracheal, and five subcarinal nodes.

As shown in Table 2, CE-CT correctly identified the nodal stage in 40 out of 57 patients (70%). Overstaging occurred in 14 patients (24%) and understaging occurred in three patients (5%). PET-CT correctly identified the nodal stage in 51 out of 57 patients (89%). Overstaging occurred in four patients (7%) and understaging occurred in two patients (3%).

N1 and N2 diseases were combined as N+ disease to compare diagnostic efficacy of CE-CT and PET-CT in the detection of hilar and mediastinal nodal metastasis.

PET-CT correctly identified 44 out of 48 patients (92%) who did not have metastatic lymph node involvement on histological analysis (N0 disease). In the present study, four patients with false-positive PET-CT findings had pulmonary diseases including previous pulmonary tuberculosis and

Table 2. Number of patients with respect to lymph node staging by CE-CT or PET-CT and histological stage

	CE-CT Stage				PET-CT Stage			
Histological staging	N0	N1	N2	Total	N0	N1	N2	Total
Correct	35	3	2	40	44	3	4	51
Overstaged	13	0	1	14	4	0	0	4
Understaged	0	2	1	3	0	2	0	2
Total	48	5	4	57	48	5	4	57

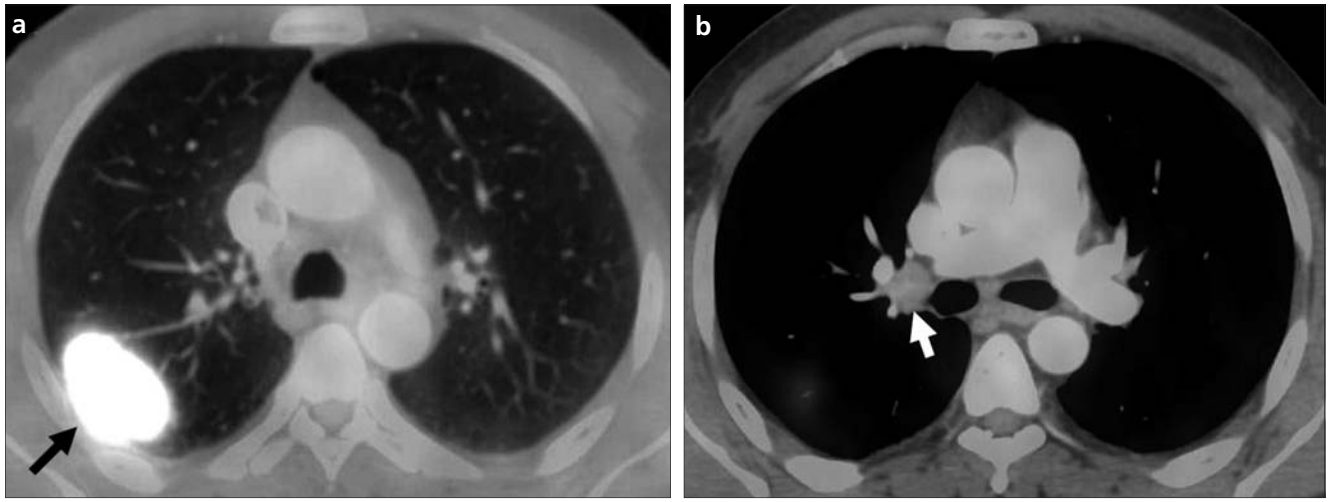

Figure 1. a, b. A 48-year-old man with adenocarcinoma in the right upper lobe. Axial fused PET-CT scan **(a)** shows a mass (*arrow*) in the right upper lobe with markedly increased FDG uptake (SUV_{max}, 10). Axial fused PET-CT scan **(b)** demonstrates no FDG uptake in a right hilar enlarged lymph node (*arrow*). This lymph node was interpreted as nodal metastasis on CE-CT. Histopathological analysis did not reveal lymph node involvement (N0 disease).

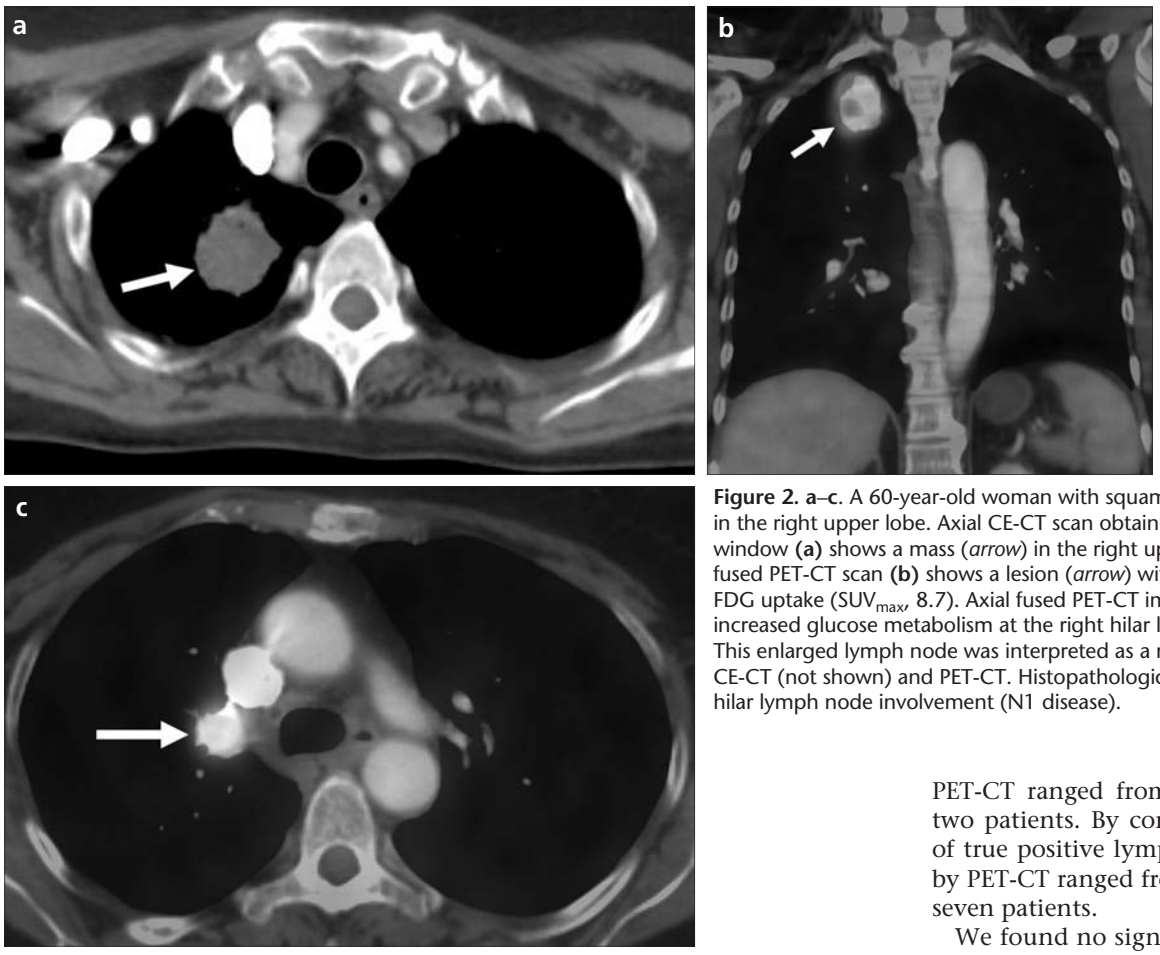

Figure 2. a–c. A 60-year-old woman with squamous cell carcinoma in the right upper lobe. Axial CE-CT scan obtained with mediastinal window **(a)** shows a mass (*arrow*) in the right upper lobe. Coronal fused PET-CT scan **(b)** shows a lesion (*arrow*) with markedly increased FDG uptake (SUV_{max}, 8.7). Axial fused PET-CT image **(c)** depicts increased glucose metabolism at the right hilar lymph node (*arrow*). This enlarged lymph node was interpreted as a nodal metastasis on CE-CT (not shown) and PET-CT. Histopathological analysis revealed hilar lymph node involvement (N1 disease).

silicoanthracosis. N0 disease was correctly detected by CE-CT in 35 of 48 patients (73%). There was a significant difference between CE-CT and PET-CT for nodal staging of N0 disease ($P < 0.05$) (Fig. 1). However, metastatic lymph node involvement (N+ disease) was correctly detected by PET-CT in seven out of nine patients (78%) and by CE-CT in five out of nine patients (56%) (Fig. 2). The size of false-negative lymph nodes identified through PET-CT ranged from 5 to 10 mm in two patients. By comparison, the size of true positive lymph nodes detected by PET-CT ranged from 8 to 32 mm in seven patients.

We found no significant differences between CE-CT and PET-CT for staging of N+ disease ($P > 0.05$). CE-CT showed an overall sensitivity of 56%, a specificity of 73%, a positive predictive value of 28%, a negative predictive value of 90%, and an accuracy of 70% for the detection of nodal metastases on a per-patient basis. The

results for PET-CT were as follows: sensitivity, 78%; specificity, 92%; positive predictive value, 64%; negative predictive value, 96%; and accuracy, 89% (Table 3).

The mean diameters of the primary lung tumors were 3.2 cm in N0 disease and 4.6 cm in N+ disease. We found a statistically significant correlation between the tumor size and lymph node metastasis ($P = 0.03$).

There was no significant relationship between the SUV_{max} of lung cancer and lymph node metastasis ($P > 0.05$).

Discussion

The primary goal of staging lung cancer is to select patients who are likely to benefit from surgery. The role of integrated PET-CT has been investigated as a noninvasive staging modality in patients with NSCLC. In the early literature, PET-CT showed substantially higher accuracy in overall tumor staging compared with CT and PET used separately (5, 10, 12, 16, 17). Our results were consistent with these reports and showed that the sensitivity, specificity, positive predictive value, negative predictive value, and accuracy of PET-CT were superior to those of CE-CT in mediastinal and hilar node staging in NSCLC. Reported sensitivities and specificities of CT for lymph node staging in patients with NSCLC range from 50% to 66% and from 65% to 94%, respectively (18–20). In our study, the CE-CT diagnostic efficacy for the identification of nodal metastasis was based on sensitivity (56%), specificity (73%), positive predictive value (28%), negative predictive value (90%), and accuracy (70%). Our results were consistent with previously reported observations. In the present study, the positive predictive value of CE-CT was lower than previously reported. Out of the 57 consecutive patients, 14 patients (24%) were falsely overstaged. False-positive CE-CT findings have been related to lymph node enlargement due to benign processes. A limitation of CE-CT in staging of hilar and mediastinal lymph node involvement is that lymph node metastases are assessed only on the basis of nodal size.

By allowing the simultaneous registration of spatially matched metabolic and anatomic data, PET-CT was thought to be particularly helpful for identifying metastatic deposits in normal-sized lymph nodes and for distinguishing between hyperplastic lymph nodes and enlarged metastatic lymph nodes. The limitations of the spatial and anatomic resolution continue to be the main factors for false-negative results of PET-CT.

Shim et al. (4) reported that for the depiction of malignant nodes, including mediastinal and hilar nodal groups, the sensitivity, specificity, and accuracy of CT were 70%, 69%, and 69%, respectively, whereas those of PET-CT were 85%, 84%, and 84%, respectively. However, according to a study by Kim et al. (5) the sensitivity, specificity, positive predictive value, negative predictive value, and accuracy of PET-CT for hilar and mediastinal nodal staging were 47%, 100%, 100%, 87%, and 88%, respectively, in stage T1 NSCLC.

More recently, the improved accuracy and sensitivity of PET-CT have been confirmed by several studies (10, 12). Although our results showed that integrated PET-CT was more useful than CE-CT for lymph node staging, the sensitivity (78%) and positive predictive value (64%) of PET-CT were lower than previously reported. One possible reason for these relatively low values is the difference in the inclusion criteria that were used. In the present study, only patients who underwent surgical treatment with lymph node dissection were included. Patients who received palliative treatment, pre-operative chemotherapy, or radiation therapy were excluded.

In our study, PET-CT was characterized by a 96% negative predictive value in the detection of hilar and mediastinal lymph nodes. We found a significant difference between CE-CT and PET-CT for nodal staging of N0 disease ($P < 0.05$). These values suggest that a diagnosis of N0 disease with PET-CT does not require additional verification with mediastinal lymph node mapping. However, noting that false-positive results were obtained in four patients in our series, one should use caution when interpreting the positive predictive value of PET-CT. Based on our study results, we propose, for diagnostic and treatment purposes, that mediastinoscopy should be performed to confirm the presence of N+ disease when PET-CT suggests the presence of hilar and mediastinal nodal metastasis. False-positive FDG uptake can be caused by pulmonary tuberculosis, silicoanthracosis, and physiologic uptake.

The tumor size significantly influenced the incidence of malignant mediastinal adenopathy, with larger tumors being more likely to have nodal involvement than smaller tumors. Our results agree with many previous studies that showed a higher risk with increased tumor size (8, 21). The larger the primary tumor, the greater is the likelihood that it has metastasized to lymph nodes.

Many previous studies concluded that the likelihood of lymph node metastasis increases with an increase in SUV_{max} of the primary tumor (22, 23). Our results are not consistent with those observations. We found no significant relationship between the SUV_{max} of lung cancer and lymph node metastasis ($P > 0.05$). However, there was a significant relationship between the SUV_{max} of lung cancer and tumor size ($P < 0.05$) in our study. We concluded that larger primary tumors led to higher SUV_{max} of lung cancer.

Our study has several limitations. Our study population consisted only of patients who underwent surgery, whereas patients who were inoperable due to advanced stages had been excluded. Another limitation is that our study was not designed prospectively, which may have resulted in selection bias. Finally, hilar and mediastinal nodal metastases were calculated based on a relatively small number of patients. This must be duly considered when interpreting the data.

PET-CT has some limitations. Firstly, PET-CT is more expensive than CE-CT. The current Medicare reimbursement

Table 3. Overall accuracy of detection of lymph node metastasis through CE-CT and PET-CT in patients with NSCLC

	Sensitivity	Specificity	Positive predictive value	Negative predictive value	Accuracy
CE-CT	56%	73%	28%	90%	70%
PET-CT	78%	92%	64%	96%	89%

for whole-body PET-CT is approximately $2000 in the USA and 1030 TL (approximately $550) in Turkey. Secondly, the effective dose for FDG is 10 mSv from 370 MBq FDG. Depending on the specific CT protocol and the FDG activity, the equivalent effective dose for whole-body PET-CT may range between 10 mSv and 25 mSv.

In conclusion, our study showed that integrated PET-CT was more accurate than CE-CT in lymph node staging of NSCLC. However, both the published literature and our experience underline the continued need for tissue confirmation of a positive PET-CT result during evaluation for mediastinal lymph node involvement in patients with clinically resectable NSCLC to determine whether patients are candidates for potentially curative surgery or for protocols involving induction therapy.

Conflict of interest disclosure

The authors declared no conflicts of interest.

References

1. Cerfolio RJ, Bryant AS, Ohja B, Bartolucci AA. The maximum standardized uptake values on positron emission tomography of a non-small cell lung cancer predict stage, recurrence, and survival. J Thorac Cardiovasc Surg 2005; 130:151–159.
2. Konishi J, Yamazaki K, Tsukamoto E, et al. Mediastinal lymph node staging by FDG-PET in patients with non-small cell lung cancer: analysis of false-positive FDG-PET findings. Respiration 2003; 70:500–506.
3. Bille A, Pelosi E, Skanjeti A, et al. Preoperative intrathoracic lymph node staging in patients with non-small-cell lung cancer: accuracy of integrated positron emission tomography and computed tomography. Eur J Cardiothorac Surg 2009; 36:440–445.
4. Shim SS, Lee KS, Kim BT, et al. Nonsmall cell lung cancer: prospective comparison of integrated FDG PET/CT and CT alone for preoperative staging. Radiology 2005; 236:1011–1019.
5. Kim BT, Lee KS, Shim SS, et al. Stage T1 non-small cell lung cancer: preoperative mediastinal nodal staging with integrated FDG PET/CT—a prospective study. Radiology 2006; 241:501–509.
6. Kim YK, Lee KS, Kim BT, et al. Mediastinal nodal staging of nonsmall cell lung cancer using integrated 18F-FDG PET/CT in a tuberculosis-endemic country: diagnostic efficacy in 674 patients. Cancer 2007; 109:1068–1077.
7. An YS, Sun JS, Park KJ, et al. Diagnostic performance of 18F-FDG PET/CT for lymph node staging in patients with operable non-small-cell lung cancer and inflammatory lung disease. Lung 2008; 186:327–336.
8. Higashi K, Ito K, Hiramatsu Y, et al. 18F-FDG uptake by primary tumor as a predictor of intratumoral lymphatic vessel invasion and lymph node involvement in non-small cell lung cancer: analysis of a multicenter study. J Nucl Med 2005; 46:267–273.
9. Yi CA, Lee KS, Kim BT, et al. Efficacy of helical dynamic CT versus integrated PET/CT for detection of mediastinal nodal metastasis in non-small cell lung cancer. AJR Am J Roentgenol 2007; 188:318–325.
10. Lardinois D, Weder W, Hany TF, et al. Staging of non-small-cell lung cancer with integrated positron-emission tomography and computed tomography. N Engl J Med 2003; 348:2500–2507.
11. Takamochi K, Yoshida J, Murakami K, et al. Pitfalls in lymph node staging with positron emission tomography in non-small cell lung cancer patients. Lung Cancer 2005; 47:235–242.
12. Antoch G, Stattaus J, Nemat AT, et al. Nonsmall cell lung cancer: dual-modality PET/CT in preoperative staging. Radiology 2003; 229:526–533.
13. Shin KM, Lee KS, Shim YM, et al. FDG PET/CT and mediastinal nodal metastasis detection in stage T1 non-small cell lung cancer: prognostic implications. Korean J Radiol 2008; 9:481–489.
14. AJCC cancer staging manual. 6th ed. New York, NY: Springer, 2002; 165–177.
15. Mountain CF, Dresler CM. Regional lymph node classification for lung cancer staging. Chest 1997; 111:1718–1723.
16. Cerfolio RJ, Ojha B, Bryant AS, Raghuveer V, Mountz JM, Bartolucci AA. The accuracy of integrated PET/CT compared with dedicated PET alone for the staging of patients with non-small cell lung cancer. Ann Thorac Surg 2004; 78:1017–1023.
17. Halpern BS, Schiepers C, Weber WA, et al. Presurgical staging of non-small cell lung cancer. Positron emission tomography, integrated positron emission tomography/CT, and software image fusion. Chest 2005; 128:2289–2297.
18. Seely JM, Mayo JR, Miller RR, Muller NL. T1 lung cancer: prevalence of mediastinal lymph node metastases and diagnostic accuracy of CT. Radiology 1993; 186:129–132.
19. Steinert HC, Hauser M, Allemann F, et al. Non-small cell lung cancer: nodal staging with FDG PET versus CT with correlative lymph node mapping and sampling. Radiology 1997; 202:441–446.
20. Von Haag DW, Follette DM, Roberts PF, Shelton D, Segel LD, Taylor T. Advantages of positron emission tomography over computed tomography in mediastinal staging of non-small cell lung cancer. J Surg Res 2002; 103:160–164.
21. Takamochi K, Nagai K, Suzuki K, Yoshida J, Ohde Y, Nishiwaki Y. Clinical predictions of N2 disease in non-small cell lung cancer. Chest 2000; 117:1577–1582.
22. Nambu A, Kato S, Sato Y, et al. Relationship between maximum standardized uptake value (SUVmax) of lung cancer and lymph node metastasis on FDG-PET. Ann Nucl Med 2009; 23:269–275.
23. Berghmans T, Dusart M, Paesmans M, et al. Primary tumor standardized uptake value (SUVmax) measured on fluorodeoxyglucose positron emission tomography (FDG-PET) is of prognostic value for survival in non-small cell lung cancer (NSCLC): a systematic review and meta-analysis (MA) by the European Lung Cancer Working Party for the IASLC Lung Cancer Staging Project. J Thorac Oncol 2008; 3:6–12.